N. Taepavarapruk, P. Taepavarapruk, J. John, Y. Y. Lai, J. M. Siegel, A. G. Phillips, S. A. McErlane and P. J. Soja

You might find this additional information useful...

This article cites 53 articles, 19 of which you can access free at:
http://jn.physiology.org/cgi/content/full/100/2/598#BIBL

This article has been cited by 1 other HighWire hosted article:

Depression of Spinal Sensory Transmission During REM Sleep: Dopaminergic Involvement and Insights Into Restless Legs Syndrome. Focus on "State-Dependent Changes in Glutamate, Glycine, GABA, and Dopamine Levels in Cat Lumbar Spinal Cord"
S. Hochman
J Neurophysiol, August 1, 2008; 100 (2): 549-550.
[Full Text] [PDF]

Updated information and services including high-resolution figures, can be found at:
http://jn.physiology.org/cgi/content/full/100/2/598

Additional material and information about *Journal of Neurophysiology* can be found at:
http://www.the-aps.org/publications/jn

This information is current as of August 13, 2008 .

State-Dependent Changes in Glutamate, Glycine, GABA, and Dopamine Levels in Cat Lumbar Spinal Cord

N. Taepavarapruk,[1] P. Taepavarapruk,[3] J. John,[4] Y. Y. Lai,[4] J. M. Siegel,[4] A. G. Phillips,[2] S. A. McErlane,[1] and P. J. Soja[1]

[1]*Faculty of Pharmaceutical Sciences and* [2]*Department of Psychiatry, Faculty of Medicine, University of British Columbia, Vancouver, British Columbia, Canada;* [3]*Department of Physiology, Faculty of Medical Science, Naresuan University, Phitsanulok, Thailand; and* [4]*Department of Psychiatry, School of Medicine, University of California, Los Angeles, and Sepulveda Veterans Affairs Medical Center, North Hills, California*

Taepavarapruk N, Taepavarapruk P, John J, Lai YY, Siegel JM, Phillips AG, McErlane SA, Soja PJ. State-dependent changes in glutamate, glycine, GABA, and dopamine levels in cat lumbar spinal cord. *J Neurophysiol* 100: 598–608, 2008. First published March 19, 2008; doi:10.1152/jn.01231.2007. Recent studies have indicated that the glycine receptor antagonist strychnine and the γ-aminobutyric acid type A (GABA$_A$) receptor antagonist bicuculline reduced the rapid-eye-movement (REM) sleep-specific inhibition of sensory inflow via the dorsal spinocerebellar tract (DSCT). These findings imply that the spinal release of glycine and GABA may be due directly to the REM sleep-specific activation of reticulospinal neurons and/or glutamate-activated last-order spinal interneurons. This study used in vivo microdialysis and high-performance liquid chromatography analysis techniques to provide evidence for these possibilities. Microdialysis probes were stereotaxically positioned in the L$_3$ spinal cord gray matter corresponding to sites where maximal cerebellar-evoked field potentials or individual DSCT and nearby spinoreticular tract (SRT) neurons could be recorded. Glutamate, glycine, and GABA levels significantly increased during REM sleep by approximately 48, 48, and 14%, respectively, compared with the control state of wakefulness. In contrast, dopamine levels significantly decreased by about 28% during REM sleep compared with wakefulness. During the state of wakefulness, electrical stimulation of the nucleus reticularis gigantocellularis (NRGc) at intensities sufficient to inhibit DSCT neuron activity, also significantly increased glutamate and glycine levels by about 69 and 45%, respectively, but not GABA or dopamine levels. We suggest that the reciprocal changes in the release of glutamate, glycine, and GABA versus dopamine during REM sleep contribute to the reduction of sensory inflow to higher brain centers via the DSCT and nearby SRT during this behavioral state. The neural pathways involved in this process likely include reticulo- and diencephalospinal and spinal interneurons.

INTRODUCTION

Recording studies performed in chronic, unanesthetized animal preparations have demonstrated that sensory transmission through the dorsal spinocerebellar tract (DSCT) and spinoreticular tracts (SRT) is subjected to dynamic, behavioral state-dependent modulation. Specifically, during the state of rapid-eye-movement (REM) sleep, the spontaneous activity, glutamate-driven activity, and sciatic nerve-evoked mono- and polysynaptic spike responses of these sensory tract neurons are inhibited compared with wakefulness or non-REM (NREM) sleep (Soja et al. 1996, 2001a,b; Taepavarapruk et al. 2002,

2004). These findings suggest that the inhibitory neurotransmitters glycine and γ-aminobutyric acid (GABA) mediate the suppression of sensory inflow through ascending sensory pathways and contribute to the sensory deafferentation of higher brain centers that occurs during REM sleep.

Although previous studies performed in "acute" anesthetized animal preparations have demonstrated an increased release of glycine and GABA in the lumbar spinal cord of animals in response to manipulations of afferent (Linderoth et al. 1994; Sorkin and McAdoo 1993) or bulbospinal pathways (Kodama et al. 2003; Sorkin et al. 1993), changes in the release of these neurotransmitters as a function of naturally occurring sleep and wakefulness in chronically instrumented behaving animals have yet to be investigated. If glycine and GABA levels are found to increase in lumbar spinal gray matter during REM sleep, conceivably this may occur via inhibitory reticulospinal neurons and/or reticulospinal activation of last-order spinal inhibitory interneurons. Microdialysis studies are thus essential for providing evidence to support these possibilities (Werman 1966). Accordingly, we used in vivo microdialysis techniques to test the hypothesis that glutamate, glycine, and GABA levels in the upper lumbar spinal cord near Clarke's column, where DSCT and SRT neurons are recorded, increase during the state of REM sleep. Complementary microdialysis studies were also performed to determine whether electrical stimulation of the nucleus reticularis gigantocellularis (NRGc) in the medullary reticular formation, an area known to produce strychnine-sensitive motoneuron inhibition during REM sleep (Chase et al. 1986; Soja et al. 1987), and the inhibition of DSCT and SRT neurons in acute decerebrate or anesthetized cats (Chandler et al. 1989; Kubota and Poppele 1977) were also capable of increasing spinal levels of these amino acids.

Moreover, given the emergent interest in state-related sensorimotor disorders such as restless legs syndrome (RLS) and the alleged dysfunctional spinal release of dopamine as one potential causative factor underlying the lower limb dysesthesias of RLS, we also determined, for the first time, whether dopamine levels in the spinal cord remained static during the transition between quiet wakefulness and NREM sleep and/or REM sleep. It is during sleep onset, in particular, that uncomfortable dysesthesias due to impaired dopamine inhibition of sensory processing occurs in RLS patients. Confirmation of a

---

state-dependent release of dopamine in the spinal cord would also provide a provenance for future investigations focusing on possible state-dependent changes in the activity of descending dopaminergic neurons. The results obtained indicate that in intact behaving, chronically instrumented cats, reciprocal changes occur in the release of amino acid versus dopamine neurotransmitters in the midlumbar gray matter and these changes occur during REM sleep when ascending sensory inflow is attenuated and motor outflow is abolished.

METHODS

Animal preparation

The chronically instrumented intact cat preparation used in these studies provided optimal conditions for assessing the levels of spinal cord neurotransmitters during naturally occurring episodes of wakefulness and sleep. This preparation has been used extensively to examine the neural mechanisms of atonia and myoclonia during naturally occurring REM sleep (Chase and Morales 1990), as well as the inhibition of spinal cord proprioceptive DSCT or nociceptive SRT neuron pathways during REM sleep compared with wakefulness (Soja et al. 1996, 2001a,b; Taepavarapruk et al. 2002, 2004). The chronic animal preparation requires the permanent implantation of electrodes for recording behavioral state as well as permanent implantation of head- and lumbar-restraining devices that permit stabilization of the neuraxis essential for long-term extracellular recordings of identified spinal neurons and/or microdialysis of neurotransmitters.

All surgical and experimental procedures reported in this study were performed on a total of three adult cats and complied with (inter)national [Canadian Council on Animal Care (http://www.ccac.ca), National Research Council (http://grants1.nih.gov/grants/olaw/olaw.htm)] and institutional (University of British Columbia Animal Care Committee) guidelines and were supervised directly by a licensed veterinarian (SAM).

Surgical implant procedures

During each of two separate surgical procedures, the animals were maintained under a deep surgical plane of anesthesia (45–60% N_2O in 1.5–2.5% halothane/oxygen mixture, 3 l/min). Heart rate/rhythm, respiratory rate, pulse oximetry, end tidal CO_2, and body temperature were continuously monitored and kept within normal physiological limits by the veterinarian (SAM) to ensure a stable, smooth, and adequate plane of anesthesia. The veterinarian also monitored for hydration status, jaw tone, eye position, pupil size, blink reflex, and withdrawal response to pinch as additional criteria for maintaining a stable surgical plane of anesthesia. Lactated Ringer solution was administered intravenously (iv) at a rate of 10 ml·kg^{-1}·h^{-1} to ensure proper hydration. The veterinarian supervised each animal's recovery from all surgical and anesthetic procedures and provided all appropriate postoperative analgesia and nursing care. Each animal recovered in a comfortable, stress-free, and pain-free environment.

Briefly, in the first procedure, electrodes for recording behavioral state were implanted into the frontal sinus [electroencephalogram (EEG)], lateral geniculate nucleus of the thalamus [pontogeniculooccipital (PGO) wave activity], the orbital plate [electrooculogram (EOG)], and neck muscles [electromyogram (EMG)]. Through the use of these electrodes, each animal's behavioral states of wakefulness and sleep could be determined. All electrode leads were connected to a 20-pin connector plug that was externalized and bonded together in a low-profile acrylic head-restraining device that was permanently affixed to the calvarium. The head-restraining device also permitted painless stereotaxic head placement during wake–sleep sessions after the animal had fully recovered. In addition, the head-restraining device permitted the investigators' access to certain brain targets. Low-intensity stimuli were applied to the

anterior cerebellar lobule and NRGc. Stimuli applied to these sites were required for locating or conditioning Clarke's column (CC) and the NRGc, respectively, during spinal dialysis procedures.

In the second procedure the L_1–L_5 vertebrae were exposed and cleaned; titanium screws were then threaded into the articulating surfaces. The animal's head, trunk, and limb postures were adjusted to approximate a natural sitting sphinx position determined previously for each animal. Then, the titanium screws were permanently tightened to secure the lumbar vertebral column. This positioning procedure ensured that the animal remained comfortable during subsequent restraint and recording/dialysis sessions. The cleaned vertebral surfaces, screws, and restraining device were dried and bonded together with dental acrylic. A chamber was fashioned in the acrylic, providing microelectrode or microdialysis probe access to the dorsal lamina of L_3–L_4 (Soja et al. 1995a).

A complete recovery over a 2.5-mo period was required before any microdialysis experiments were performed. During this recovery period, chronically instrumented animals were gradually adapted to painless head and lumbar restraint while cycling across wakefulness and sleep states. Three days prior to performing dialysis experiments and under gaseous anesthesia, a small trephination (1.5-mm diameter) was made in the dorsal surface of the L_3 vertebra, which was assessable in the lumbar recording chamber implanted previously (Soja et al. 1995a). A small trephination (2 mm) was also made in the calvarium overlying the cerebellum. The dura mater at each site was cut and the trephination covered with antibiotic crème (Neosporin, Johnson & Johnson) and the access well sealed with sterile bone wax between experimental dialysis sessions. Further details of all postsurgical recovery, daily maintenance, and restraint imprinting procedures can be found in Soja et al. (1995a).

Procedures for the in situ positioning of the microdiaylsis probe in L_3 spinal cord gray matter
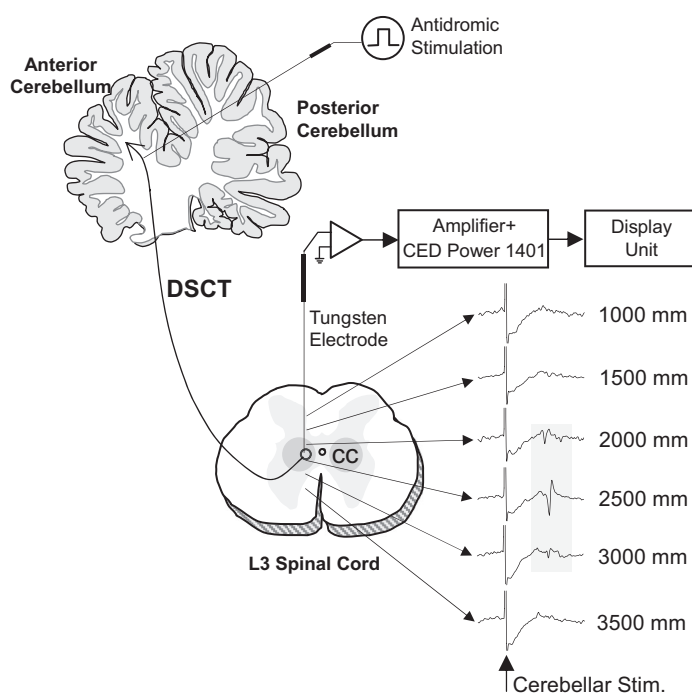
Prior to the beginning of each experimental microdialysis session, the location of Clarke's column in the L_3 spinal segment was confirmed electrophysiologically by recording characteristic short-latency (2.9–3.2 ms) field potentials or individual DSCT neurons evoked by low-intensity stimulation (0.05 ms, 0.5 Hz, 100–300 μA) of the anterior lobe of the cerebellum using a removable stimulating electrode (Cat. No. 575300, 5 MΩ, AC, A-M Systems, Carlsborg, WA) (Fig. 1A; see also Figs. 2 and 3 in Soja et al. 1995a and Fig. 1 in Soja et al. 1996). The tip of the recording electrode denoting the location of CC was then recorded. The recording electrode was carefully withdrawn and replaced with a microdialysis probe (Model A-I-40-01, Eicom, Kyoto, Japan). The probe tip was finally positioned 2,500 microns ventral to the spinal cord depths where maximal amplitude cerebellar-evoked field potentials or DSCT neurons were recorded previously and allowed to equilibrate for ≥3 h (Fig. 1C). SRT neurons are located just ventral to DSCT neurons (Soja et al. 2001b) and would be in close apposition to the tip of the microdialysis probe, allowing neurotransmitter release near SRT neurons to be assessed as well.

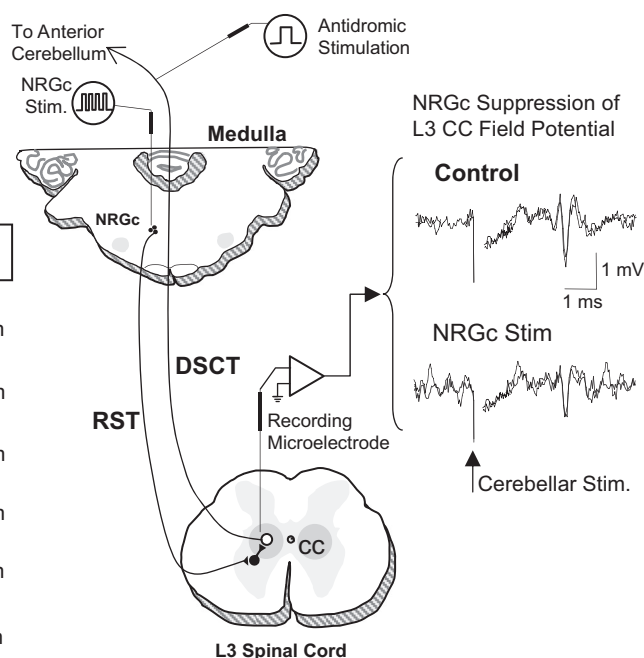### Recording and identification of behavioral state in conjunction with dialysis procedures

Behavioral state was continuously monitored during experimental microdialysis sessions. Each behavioral state (Fig. 2A) was identified using criteria identical to those used previously (Soja et al. 1996). Wake–sleep cycles were defined by consecutively occurring periods of wakefulness, NREM sleep, REM sleep, and awakening directly from REM sleep (Soja et al. 1996), which are subsequently briefly defined and illustrated in Fig. 2A.

WAKEFULNESS. The behavioral state of wakefulness was characterized by a desynchronized cortical EEG pattern, tonic EMG activity,

A   Location of Clarke's Column

B   NRGc Conditioning
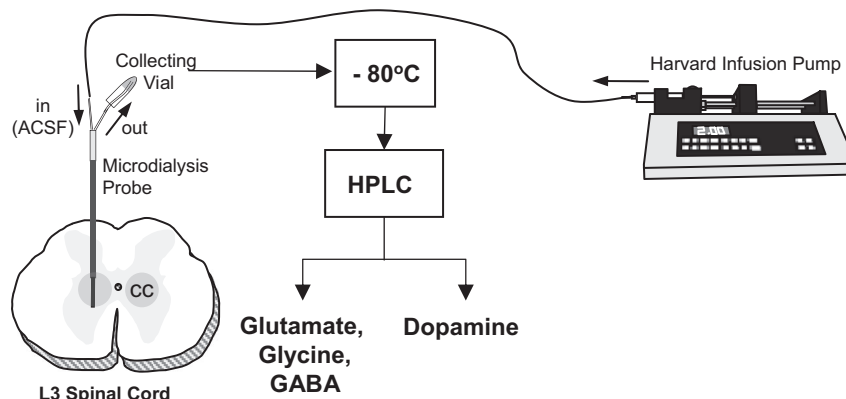

C   Spinal Microdialysis

FIG. 1. Experimental scheme illustrating procedures used for locating Clarke's column (CC) at the L_3 spinal cord segment (*A*), optimal site for conditioning the nucleus reticularis gigantocellularis (NRGc) in the medulla oblongata (*B*), and sampling spinal dialysates from CC (*C*). The location of CC was determined by monitoring maximal amplitude field potentials evoked by stimulation of the anterior cerebellar lobule (*A*). Conditioning stimuli were applied to the NRGc at intensities sufficient to suppress cerebellar-evoked field potentials via the reticulospinal pathway (RST) (*B*). The tip of the microdialysis probe placement in CC corresponded to stereotaxic coordinates 2,500 microns ventral to where maximal cerebellar field potentials were recorded. The dialysate in each collecting vial was stored at −80°C before high-performance liquid chromatography (HPLC) analyses (*C*; see METHODS for further details).

sparse PGO wave activity, and the presence of EOG wave activity. During wakefulness, few postural movements occurred.

NREM SLEEP.   The behavioral state of NREM sleep (also known as quiet sleep; Soja et al. 1991, 1996) was characterized by a large-amplitude synchronized slow-wave EEG pattern, relatively moderate EMG activity, and little or no EOG and PGO wave activity.

REM SLEEP.   REM sleep (also known as active sleep; Soja et al. 1991, 1996) was characterized by a "desynchronized," high-frequency, low-amplitude EEG waveform pattern similar to the EEG signature of wakefulness. In addition, muscle atonia indicated by flat, isoelectric EMG activity, robust PGO wave activity, and clustered EOG activity verified the state of REM sleep. The latter two parameters, PGO and EMG, occurred in phasic bursts and designated phasic eye movement events characteristic of the REM sleep state.

AWAKENING FROM REM SLEEP.   When the animals awakened from REM sleep, EEG, EMG, PGO, and EMG activities returned back to their same corresponding patterns recorded in the previous state of wakefulness.

Each chronically instrumented cat preparation readily cycled between wakefulness and sleep during each experimental microdialysis session, which typically lasted 6–7 h. Microdialysis sessions were performed during the midafternoon, 2 days/wk.

Spinal microdialysis and HPLC

Microdialysis probes used in all experiments were concentric and consisted of polyimide-resin–coated fused silica (ID: 0.20 mm; OD: 0.35 mm), stainless steel (ID: 0.12 mm; OD: 0.18 mm), and a cellulose membrane (ID: 0.20 mm; OD: 0.22 mm; 50K Da molecular
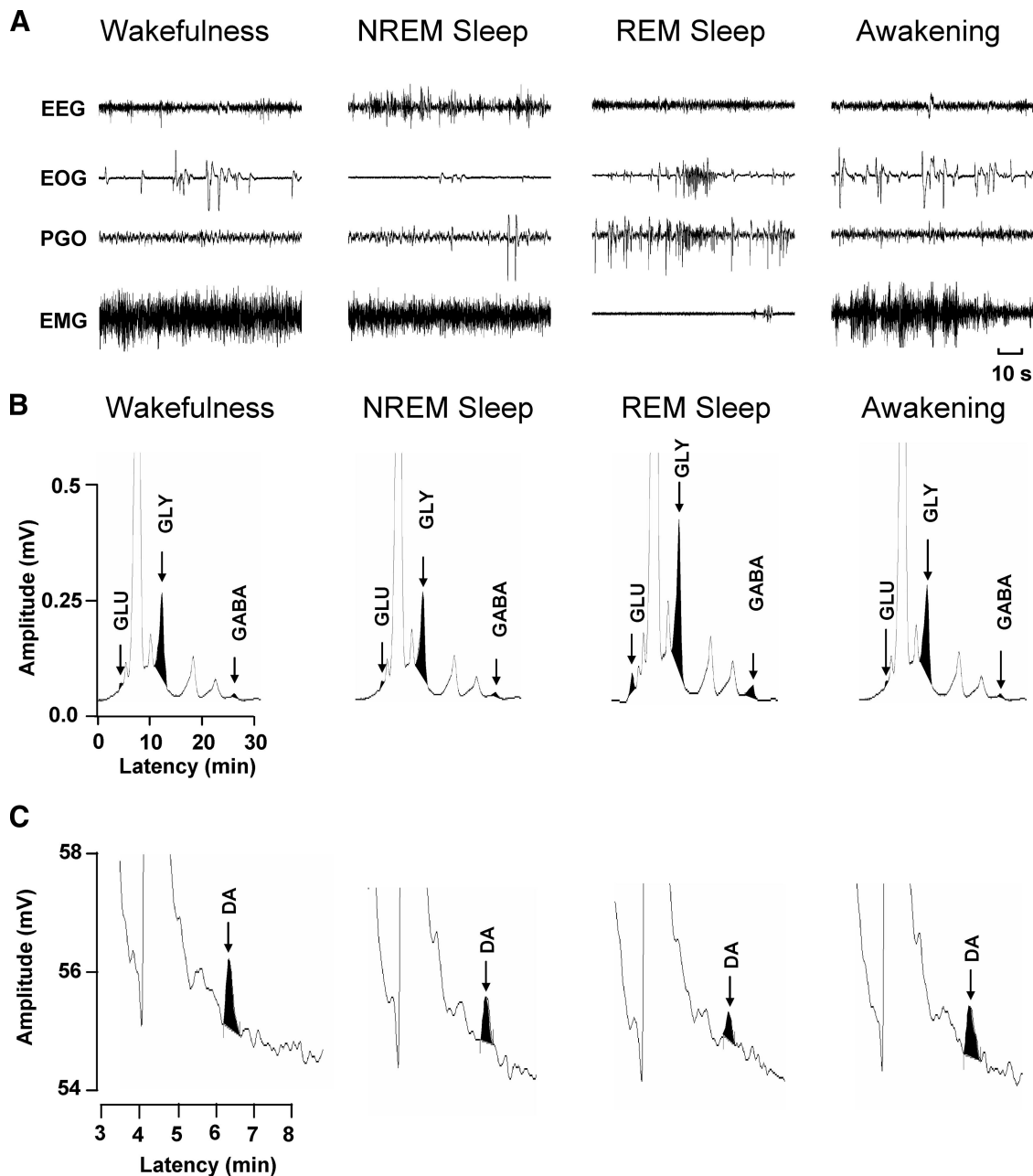
FIG. 2. Examples of HPLC chromatograms of the amino acid neurotransmitters, glutamate (GLU), glycine (GLY), γ-aminobutyric acid (GABA), as well as dopamine (DA) during wakefulness and sleep. Behavioral states of wakefulness, nonrapid-eye-movement (NREM) sleep, rapid-eye-movement (REM) sleep, and awakening are indicated by 1.5-min continuous records of electroencephalographic (EEG), electrooculographic (EOG), pontogeniculooccipital (PGO), and electromyographic (EMG) activities (A). A relatively short 1.5-min time period is depicted to clearly illustrate the characteristic and marked differences in EEG, EOG, PGO, and EMG activities that were routinely used to score behavioral state when spinal dialysis samples for glutamate, glycine, GABA, and dopamine were collected. The chromatograms in B illustrate the change in glutamate, glycine, and GABA. There were marked increases in each of these neurotransmitters only during REM sleep. In contrast, there was a marked decrease in dopamine levels only during REM sleep compared with the other behavioral states (C).

weight cutoff). To limit the location of dialysate sampling near Clarke's column, the length of the active membrane of the probes used in all experiments was 1 mm.

In all, 34 microdialysis probes were used in this study [18 probes were used for amino acids (glutamate, glycine, and GABA) experiments and 16 probes were used for dopamine experiments]. Prior to use, each dialysis probe was flushed with distilled water at the flow rate of 1 μl/min and the relative recovery for amino acids (glutamate, glycine, and GABA) was obtained in vitro by immersing the tip of the probe in a standard medium containing each amino acid at the concentration of 1 μM. Artificial cerebrospinal fluid (ACSF; Cat. No.

AH 59-7316, Harvard Apparatus, Holliston, MA) was infused at the flow rate of 2 μl/min for $\geq$5 min. The final ion concentrations (in mM) in ACSF were: Na 150; K 3.0; Ca 1.4; Mg 0.8; P 1.0; Cl 155. Each dialysate sample was obtained during a 5-min period in the middle of each behavioral state (i.e., wakefulness, NREM sleep, REM sleep, and awakening from REM sleep) and then stored immediately at $-80°$C for later analysis. The concentration of amino acids in the dialysate was determined by a high-performance liquid chromatograph (HPLC) equipped with a fluorescent detector system, whereas that of dopamine was determined by HPLC apparatus equipped with an electrochemical detector system.

After checking the relative recovery, the microdialysis probe was carefully lowered stereotaxically to Clarke's column and continuously perfused with ACSF for ≥3 h prior to experimental testing. Behavioral state was continuously monitored by observing the cat's electrophysiological indices and dialysis samples were collected during wakefulness, NREM sleep, REM sleep, and awakening from REM sleep. The 10-μl samples collected and submitted for analysis were those that corresponded to each behavioral state that extended across 16–18 wake–sleep cycles, which averaged 77 min in length (W:NREM:REM:AW = 20:40:7:10 min). Each spinal dialysate (10 μl) was collected in a polypropylene sample tube filled with preservative agent (10 μl) and then stored at −80°C immediately after the collection until HPLC analysis.

Analysis of amino acids and dopamine

The frozen dialysate (−80°C) samples were coded and divided into two groups. Those analyzed for the amino acids glutamate, glycine, and GABA were delivered by express (same day) air courier service to Dr. J. M. Siegel's research laboratories (UCLA, Sepulveda, CA), for HPLC analysis, whereas the second group to be analyzed for dopamine was delivered to Dr. A. G. Phillips's laboratories (University of British Columbia, Vancouver, Canada), for immediate HPLC analysis. The results from amino acid and dopamine assays were submitted to the Soja laboratories for decoding and further statistical analyses.

Amino acid assay

Glutamate, glycine, and GABA levels in the dialysate were determined by HPLC (EP-300, Eicom, Kyoto, Japan) with fluorescent detection (excitation/emission = 340/440 nm; LC 305, Alltech Associates, Deerfield, IL) as described in our prior studies (John et al. 2003; Kodama et al. 2003). The sample was injected using an autoinjector (ESA 540, ESA, Chelmsford, MA). Precolumn derivatization was performed with o-phthaldialdehyde/2-mercaptoethanol at 5°C for 3 min. The derivatives were then separated in a liquid chromatography column (SC-5ODS, 2.1 × 150 mm; Eicom, San Diego, CA) at 32°C with 30% methanol in 0.1 M phosphate buffer (pH 6.0), being degassed by an on-line degasser (DG-100, Eicom). Quantification was achieved with a PowerChrom analysis system (AD Instruments, Sydney, NSW, Australia) using external amino acid standards (Sigma, St. Louis, MO). Neurotransmitter concentrations were calculated by comparing the HPLC peak of amino acid in microdialysis samples with the peak area of known concentrations of the same compounds analyzed on the same day. The detection limit was 20 fmol.

Dopamine assay

Dopamine levels in the dialysate were determined using a HPLC system with electrochemical detection procedures identical to those used previously (Taepavarapruk and Phillips 2003). Briefly, the HPLC-EC system consisted of a HPLC pump (model LC1120, GBC, Victoria, Australia), a pulse damper (model 316 Stainless Steel Model; Scientific Systems, State College, PA), a Rheodyne manual injector (20 μl injection loop; Model 9125), a C_{18} column (Princeton SPHER 60A 3 μm, 2 × 100 mm; Princeton Chromatography, Cranbury, NJ), a Links system (Antec Leyden, Zoeterwoude, The Netherlands), and an Intro EC detector with a VT-03 electrochemical flow cell ($V_{applied}$ = +0.7 V; Antec Leyden). The mobile phase consisted of 6 g/l sodium acetate, 70 mg/l octyl sulfate (adjustable), 20 mg/l EDTA, 35 ml/l glacial acetic acid, and 865 ml Milli Q purified water. The mobile phase was adjusted to pH 3.5 with glacial acetic acid and filtered through a 0.22-μm sterile nylon filter unit (Millipore). Methanol (HPLC grade, 10% per volume) was added to the mobile phase solution and degassed prior to use. Dopamine was quantified from

each sample by comparing sample peak heights to peak heights from a calibration curve of the standard solution containing dopamine at three different concentrations. The limit of dopamine detection for the detector was 100 pmol/l.

Electrical stimulation of the nucleus reticularis gigantocellularis (NRGc)

A monopolar tungsten stimulating electrode (Cat. No. 575300, 5 MΩ, AC, A-M Systems) was stereotaxically placed into the NRGc (HC: P-10, L: 1.0–2, H: −6.5 to −8.5) prior to dialysis sampling (Fig. 1B). When conditioning dialysis experiments were performed, stimulus trains consisting of four pulses (0.8-ms duration, 2.5-ms interpulse interval, 120 μA) were delivered at a rate of 1.0 burst/s during a 5-min period when the animal was confirmed to be in a state of wakefulness. This level of stimulation inhibits DSCT neuron activity (Fig. 1B) and produces mixed excitatory/inhibitory postsynaptic potentials (EPSP/IPSPs) during wakefulness and NREM sleep as well as REM sleep-specific, strychnine-sensitive IPSPs in lumbar motoneurons (Chase et al. 1986; Soja et al. 1987).

Data collection and analyses

All dialysis samples were collected during the mid- to late-afternoon time period (14:00 to 18:00 h). Extracellular levels of the amino acids glutamate, glycine, GABA, and dopamine in Clarke's column were expressed as the percentage of the average of baseline value obtained during the state of wakefulness (control). The levels of amino acid neurotransmitters and dopamine were uncorrected for probe recovery. All values presented in figures are expressed as the group means ± SE (pmol/μl sample) for 18 separate wakefulness/sleep cycles conducted in three separate chronic cat preparations (6 sleep cycles/cat) for the neurotransmitters glutamate, glycine, and GABA, and for dopamine, a total of 14 separate sleep cycles.

Normality tests were performed for group mean data of transmitter levels across wakefulness/sleep states (Fig. 3) or following electrical
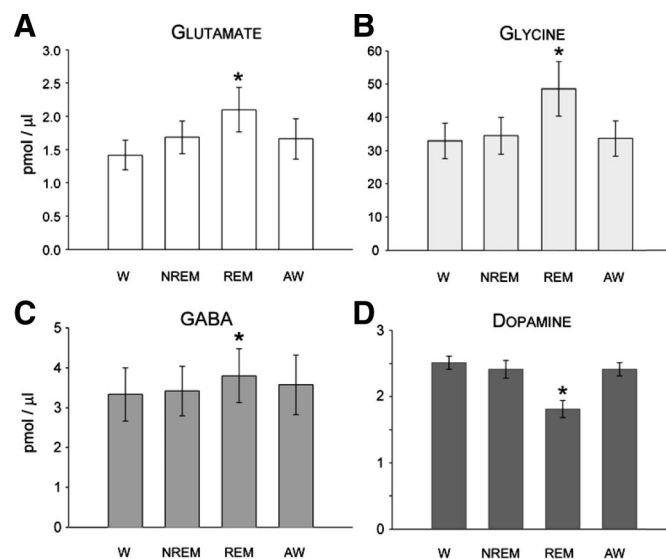
FIG. 3. State-dependent change in the levels of glutamate (A), glycine (B), GABA (C), and dopamine (D) in the L_3 spinal cord segment. Each histogram bar represents the group mean (±SE) of neurotransmitter level over 18 (A–C) and 16 (D) separate wake–sleep cycles comprised of consecutively occurring episodes of wakefulness (W), nonrapid-eye-movement sleep (NREM), rapid-eye-movement sleep (REM), and awakening from REM sleep (AW). Values obtained during W served as a control. Note that during REM sleep, glutamate, glycine, and GABA levels increased significantly by 47, 48, and 14%, respectively, whereas dopamine levels decreased by 28% (*$P < 0.05$, repeated-measures ANOVA, or Friedman repeated-measures ANOVA on ranks, Tukey test).

stimulation of the NRGc (Fig. 5) were performed and followed by one-way repeated-measures ANOVA using SigmaStat 3.1 (Systat Software, San Jose, CA). However, not all of the data reported herein (Figs. 3 and 5) were normally distributed. In such cases, absolute transmitter levels were compared during wakefulness, NREM sleep, REM sleep, and awakening from REM sleep or during wakefulness following NRGc conditioning using a nonparametric Friedman repeated-measures ANOVA on ranks to determine whether a statistical difference was present. Then, for either ANOVA result where alpha = 0.05, a multiple comparison procedure (Tukey test) was performed to isolate the group or groups that differed from the others. Changes in amino acid and dopamine levels in Clarke's column across behavioral states of wakefulness, NREM, REM, and awakening from REM sleep (Fig. 3) or around NRGc conditioning (Fig. 5) are reported in the text as relative (percentage) changes and were based on corresponding absolute control levels obtained during wakefulness.

Terminal procedures

At the termination of all experimental recording sessions, the animals were humanely killed with an anesthetic overdose (Euthanyl, 120 mg/kg, iv), perfused with saline and formalin, and the entire spinal cord section corresponding to dialysis sites and the medullary reticular formation stimulation sites was removed. Locations of the tips of dialysis probes and stimulating electrodes were verified histologically (Fig. 6).

RESULTS

Identification of the depth of Clarke's column

Figure 1A illustrates standard electrophysiological procedures used to locate the spinal gray matter area corresponding to Clarke's column in the L_3 spinal cord segment. Following a low-intensity stimulation of the anterior cerebellum, short-latency evoked (2.9–3.2 ms) field potentials could be observed (Soja et al. 1995a, 1996). The peak-to-peak amplitude was verified with the depth of the recording microelectrode. In three chronic cats, the recording depths of Clarke's column in situ ranged from 1,650 to 3,300 μm below the dorsal surface of the L_3 spinal cord. The depths where maximum amplitude field potentials were recorded were used to determine the position of the microdialysis probe tip (Fig. 1C). Overall, the depth of Clarke's column observed in this study was similar to that of previous studies (Soja et al. 1995a, 1996). The final position of the probe was 500 microns beyond the maximal depth of the recorded cerebellar-evoked field potentials. The rationale here was to also sample neurotransmitter release near SRT neurons, which are recorded just ventral to Clarke's column DSCT neurons (Soja et al. 2001a,b). Dialysate samples were collected across a total of 34 wake–sleep cycles (18 and 16 wake–sleep cycles for the assay of amino acids and dopamine, respectively) from three chronic cats. Each dialysis sample was collected during electrophysiologically confirmed states of wakefulness, NREM sleep, REM sleep, and awakening from REM sleep (Soja et al. 1995a, 1996). The mean durations ($\pm$SD) of wakefulness, NREM sleep, and REM sleep periods from a total of 34 sleep cycles (from three chronic cats) were 13.7 $\pm$ 6.5, 30.3 $\pm$ 11.2, and 5.2 $\pm$ 3.6 min, respectively.

Dialysis samples for the amino acids collected around NRGc conditioning were performed during 14 separate states of quiet wakefulness in three chronic cats.

Excitatory amino acid glutamate and inhibitory amino acids glycine and GABA

Peaks from chromatograms were used to quantify the concentration of amino acids glutamate, glycine, and GABA. Typical chromatograms obtained from the spinal dialysates during each behavioral state are shown in Fig. 2.

GLUTAMATE. Averaged glutamate levels in Clarke's column, sampled over 18 separate wake–sleep cycles, differed significantly [Fig. 3A, $F(17,51) = 10.53$, $P < 0.001$, repeated-measures ANOVA]. A pairwise multiple-comparison Tukey test indicated that, compared with the state of wakefulness, glutamate levels were elevated by about 48% during REM sleep (q = 7.82, $P < 0.001$), whereas during NREM sleep, the glutamate increase was about 19% (q = 4.75, $P < 0.08$) and about 17% compared with awakening from REM sleep (q = 5.023, $P < 0.050$). However, glutamate levels during wakefulness did not differ from levels measured during NREM sleep or awakening from REM sleep (Figs. 2B and 3A, $P > 0.05$, repeated-measures ANOVA).

GLYCINE. Glycine levels in Clarke's column, sampled over 18 separate wake–sleep cycles in three separate cats (6 sleep cycles/cat), differed significantly (Fig. 3B, $\chi^2 = 32.09$, $P < 0.001$, Friedman repeated-measures ANOVA on ranks). A pairwise multiple-comparison Tukey test subsequently indicated that glycine levels also increased significantly during REM sleep. Figure 3B illustrates that, compared with wakefulness, glycine levels were elevated by about 48% during REM sleep (q = 7.58, $P < 0.05$) and by about 41% compared with NREM sleep (q = 5.20, $P < 0.05$). The increase in glycine levels during REM sleep measured about 44% compared with awakening from REM sleep (q = 5.84, $P < 0.05$). As was the case for glutamate, glycine levels during wakefulness did not differ with levels measured during NREM sleep or awakening from REM sleep (Figs. 2B and 3C, $P > 0.05$, repeated-measures ANOVA).

GABA. GABA levels in Clarke's column, sampled over 18 separate wake–sleep cycles, also differed significantly (Fig. 3C, $\chi^2 = 12.07$, $P < 0.007$, Friedman repeated-measures ANOVA on ranks). GABA levels increased significantly during REM sleep by about 14% compared with wakefulness only (q = 4.75, $P < 0.05$, Tukey test). As was the case for glutamate and glycine, GABA levels during wakefulness did not differ with levels measured during NREM sleep or awakening from REM sleep (Figs. 2B and 3C, $P > 0.05$, repeated-measures ANOVA).

DOPAMINE. Typical chromatograms obtained from the spinal dopamine dialysates during each behavioral state are shown in Fig. 2C. The overall change in dopamine levels in the L_3 spinal segment across 16 wake–sleep cycles is presented in Fig. 3D. The mean ($\pm$SE) dopamine levels in Clarke's column, sampled over 16 separate wake–sleep cycles, differed significantly [Fig. 3D, $F(15,45) = 11.54$, $P < 0.001$, repeated-measures ANOVA]. A pairwise multiple-comparison Tukey test indicated that compared with the state of wakefulness, dopamine levels were reduced by about 28% during REM sleep only (q = 7.43, $P < 0.001$). Dopamine levels during wakefulness did not differ with levels measured during NREM sleep or awakening from REM sleep (Figs. 2C and 3D, $P > 0.05$, repeated-measures ANOVA).

These results indicate that in the normal, intact animal, spinal dopamine levels are diminished during the state of REM sleep, whereas the levels of glutamate, glycine, and GABA are increased.

Effects of electrical stimulation of the NRGc during wakefulness on amino acids and dopamine in the L_3 spinal cord

Previous microdialysis studies performed in decerebrate, unanaesthetized cats have shown that electrical stimulation of the pontine reticular formation culminates in reciprocal changes in the amino acids glutamate, glycine, and GABA versus the monoamines serotonin and noradrenaline or dopamine in the lower lumbar spinal cord ventral horn (Kodama et al. 2003; Lai et al. 2001). Thus complementary microdialysis studies were performed to determine whether phasic electrical stimulation of the NRGc during the state of wakefulness produces consequential changes in amino acid and dopamine levels in the lumbar spinal cord near Clarke's column akin to those during REM sleep versus wakefulness.

Electrical stimulation of the NRGc at intensities sufficient to suppress cerebellar-evoked field potentials by about 30% exerted differential effects on the L_3 levels of amino acids and dopamine. Examples of NRGc stimulation-induced changes in the chromatograms of glutamate, glycine, and GABA are presented in Fig. 4. Averaged glutamate levels in Clarke's column around NRGc conditioning in 14 separate experiments differed significantly (Fig. 5A, $\chi^2 = 22.29$, $P < 0.001$, Friedman repeated-measures ANOVA on ranks). Compared with baseline control values before NRGc conditioning, glutamate levels were significantly elevated by about 69% only during the period when stimuli were applied to the NRGc ($q = 5.58$, $P < 0.05$). Glutamate levels during the 5-, 10-, or 15-min poststimulation sampling periods were not different from baseline levels (Figs. 4 and 5A, $P > 0.05$, repeated-measures ANOVA).

Similarly, group mean glycine levels differed significantly around NRGc stimulation in the same 14 experiments where glutamate levels were also measured (Figs. 4 and 5B, $\chi^2 = 10.86$, $P < 0.028$, Friedman repeated-measures ANOVA on ranks) and a post hoc multiple-comparison test indicated that the roughly 45% increase was statistically significant only during NRGc sitmulation ($q = 4.40$, $P < 0.05$, Tukey test).

In contrast, GABA ($n = 14$ separate experiments, Figs. 4 and 5C, $P > 0.05$, repeated-measures ANOVA on ranks) or dopamine levels did not change during NRGc stimulation (three separate experiments, Fig. 5D, $P > 0.05$, repeated-measures ANOVA on ranks). These data indicate that NRGc stimulation during wakefulness results in a selective increase in glycine and glutamate levels near DSCT and SRT neurons.

Locations of dialysis probes in the L_3 spinal gray matter

Tracts left by the dialysis probes in the rostral, middle, and caudal portions of the L_3 spinal cord segment were confirmed at the conclusion of all experimental procedures and following histological preparation of the spinal cord (see METHODS). Figure 6A shows an example of the tip of a dialysis probe tract in one serial L_3 section. Figure 6B also summarizes the locations of the tips of the dialysis probe that were positioned stereotaxically in the vicinity of Clarke's column and nearby SRT neuron pool using field potentials driven by stimulation of the anterior cerebellar lobule.

DISCUSSION

In vivo microdialysis procedures have been used in acute decerebrate or anesthetized animal preparations to estimate the amount of neurotransmitter release in the spinal cord (Kodama et al. 2003; Lai et al. 2001; Pilowsky et al. 1986). The present study was performed in the chronically instrumented, intact, behaving cat preparation to estimate the levels of glutamate, glycine, GABA, and dopamine in Clarke's column and nearby
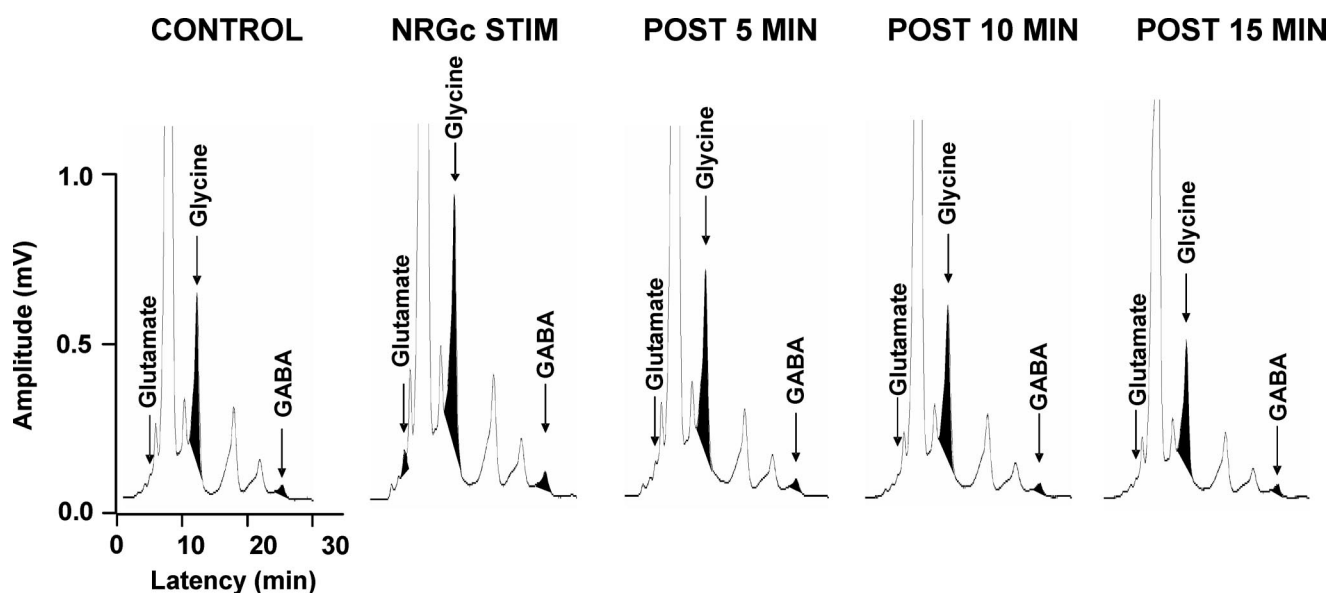

FIG. 4. Example of HPLC chromatograms illustrating elution peaks for glutamate, glycine, and GABA during control periods of wakefulness, a test period of electrical stimulation of the NRGc, and recovery from stimulation. Each chromatogram represents an individual spinal dialysate sample collected over a 5-min period. Note that electrical stimulation of the NRGc (4 pulses, 0.8-ms duration, 2.5-ms interpulse interval, 120 μA, 1.0 Hz) resulted in enhanced magnitude of amino acid signals. The NRGc-induced increase in amino acid levels in this example was transient and occurred only during the presentation of electrical stimuli.
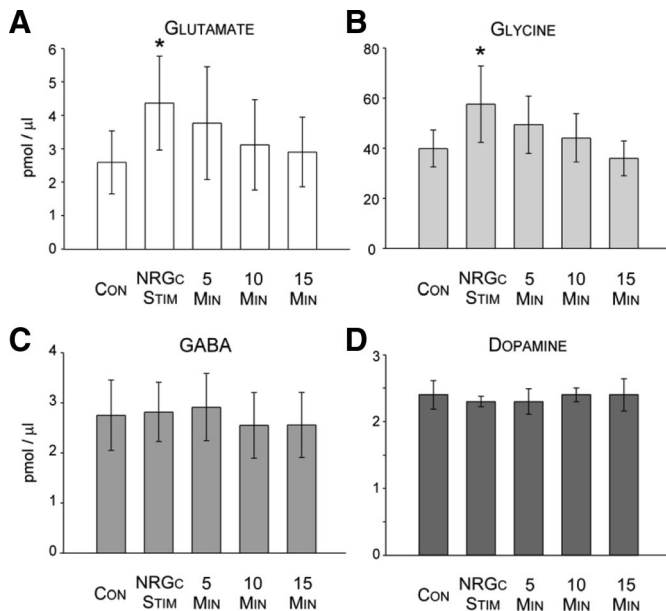
FIG. 5. Overall action of NRGc stimulation (Stim) on neurotransmitter levels in the L_3 spinal cord segment. Each histogram bar in *A* and *B* represents the group mean ($\pm$SE) level of glutamate (*A*), glycine (*B*), GABA (*C*) ($n = 14$ experiments), and dopamine (*D*, $n = 3$ experiments) during the state of wakefulness before (Con), during NRGc stimulation, and at 5-min time intervals after NRGc stimulation. Note that during NRGc stimulation, glutamate and glycine levels increased significantly by about 69 and 45%, respectively (*$P < 0.05$, repeated-measures ANOVA or Friedman repeated-measures ANOVA on ranks, Tukey test).

SRT neuron pools during the wake–sleep cycle. Compared with the control state of wakefulness, glutamate, glycine, and GABA levels increased in the L_3 spinal gray matter where Clarke's column DSCT neurons and SRT neurons are located by approximately 47, 48, and 14%, respectively, during naturally occurring REM sleep.

The only other microdialysis experiments germane to the present study were recently reported by Siegel and colleagues (Kodama et al. 2003). In their study, Kodama et al. (2003) utilized an unanaesthetized decerebrate cat preparation. They reported that motor atonia induced by the intrapontine microinjection of carbachol enhanced the spinal release of glutamate,

glycine, and GABA in the L_7 motoneuron pools by approximately 42, 50, and 65%, respectively (Kodama et al. 2003). Our findings and those of Kodama et al. (2003) suggest that certain common centrifugal pathways may be engaged during natural REM sleep to evoke the spinal release of amino acid neurotransmitters that eventuates in inhibition of spinal sensory neurons and motoneurons. The possible (supra)spinal (i.e., reticulospinal and/or spinal interneuronal) sources of these neurotransmitters and their role in regulating synaptic transmission of ascending sensorimotor information during the wake–sleep cycle are discussed in the following text.

Glutamate

The primary synaptic sources of glutamate in the spinal gray matter near Clarke's column include primary afferent terminals (Maxwell et al. 1990; Walmsley and Nicol 1991), local (inter) neurons (Buchanan and Grillner 1987), and reticulospinal neurons (Vesselkin et al. 1995). In this study, specifically during the state of REM sleep, there occurred a marked increase in L_3 spinal gray matter glutamate levels. During the state of wakefulness, in conjunction with NRGc stimulation, glutamate levels were also dramatically enhanced. It would seem unlikely that the increased levels of glutamate observed during REM sleep or NRGc stimulation emanates from group I primary afferents since monosynaptic ("glutamatergic") transmission between primary afferents and DSCT neurons is inhibited during REM sleep but not during wakefulness or NREM sleep (Taepavarapruk et al. 2004).

The dramatic increase in L_3 spinal glutamate levels during REM sleep may be due to increased activity in descending (reticulospinal) glutamatergic fibers during this state (Buchanan and Grillner 1987). Recent studies performed in chronically instrumented cats have shown that reticulospinal neurons backfired from the L_3 spinal cord increase their discharge rate during REM sleep (Taepavarapruk et al. 2003). The increase in L_3 spinal glutamate levels during REM sleep may lead to increased excitation of glycine and GABA inhibitory interneurons located in spinal segments adjacent to DSCT neurons or nearby motoneurons. The increased concentration of glutamate during NRGc stimulation may also explain the oligosynaptic
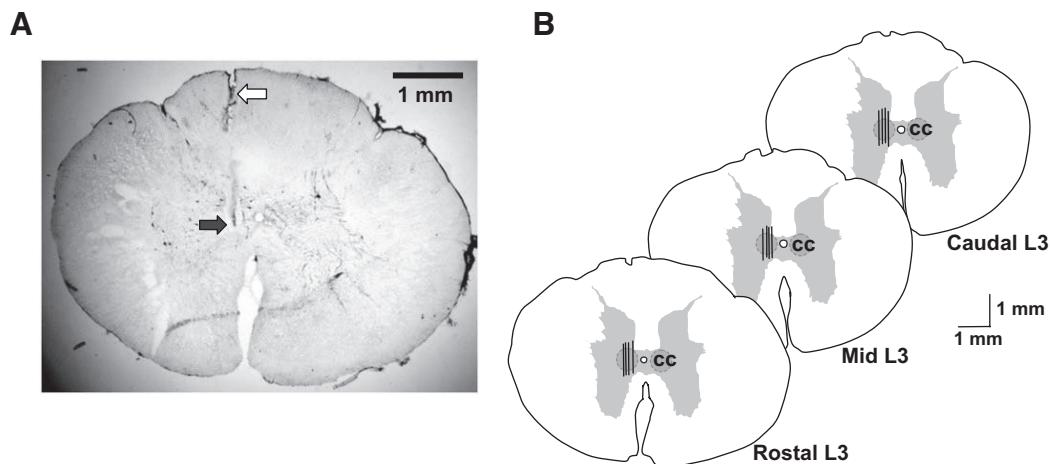

FIG. 6. *A*: histological serial section of the rostral L_3 spinal cord segment showing the tract (open arrow) and placement (filled arrow) of the tip of Eicom microdialysis probe. *B*: locations of microdialysis probes (black bars) implanted in the rostal, middle, and caudal regions of the Clarke's column nucleus (CC). Vertical lines represent the 1-mm length of dialysis membrane. The maximum field potential evoked by stimulation of the anterior cerebellar lobule corresponding to the location of Clarke's column was used as a guide for stereotaxic placement of the dialysis probes (see also Fig. 1*A*).

EPSPs recorded in lumbar motoneurons following NRGc stimulation during wakefulness or NREM sleep (Chase et al. 1986; Soja et al. 1987). Finally, during REM sleep, increased glutamate levels reported here may also partly explain the excitatory influences recorded in certain DSCT or SRT neurons (Soja et al. 1996, 2001b), or kynurenic acid-sensitive depolarization recorded intracellularly from lumbar motoneurons associated with eye movement events (Soja et al. 1995b).

Glycine and GABA

Earlier studies have established glycine and GABA as classical inhibitory neurotransmitters found throughout the spinal cord and lower brain stem (Curtis and Phillis 1958; Curtis et al. 1968). Immunocytochemical studies have also indicated high densities of glycine and GABA receptors localized in the deep dorsal and ventral gray matter (Magoul et al. 1987; Watson and Bazzaz 2001) as well as in the motoneuron pools (Ornung et al. 1994).

Another principal finding in the present study is that glycine and GABA levels in the L_3 spinal segment where DSCT and SRT neurons are recorded increase significantly during REM sleep compared with wakefulness, NREM sleep, or awakening from REM sleep. On a relative basis, the REM sleep-related increase in glycine levels was about threefold greater than that for GABA levels (i.e., 48 vs. 14%). These findings are nevertheless consistent with the idea that glycine and GABA *are* the principal inhibitory neurotransmitters (Werman 1966) that contribute to sensory deafferentation through the DSCT and SRT during this state (Soja et al. 1996, 2001a,b; Taepavarapruk et al. 2002, 2004).

It is possible that both glycinergic and GABAergic terminals originate from local or intersegmental interneurons (Curtis et al. 1986) and supraspinal sources (Holstege and Bongers 1991; Jones et al. 1991; Vesselkin et al. 1995; Wannier et al. 1995). Glycinergic inhibitory interneurons might include those cells that are thought to mediate nonreciprocal inhibition of lumbar motoneurons and DSCT neurons (Hongo et al. 1983; Rudomin et al. 1990; Takakusaki et al. 2001).

As for the identity of GABAergic interneurons, possible candidates include those neurons that might project to the area of Clarke's column and that may mediate presynaptic and postsynaptic inhibition (Solodkin et al. 1984). Alternatively, the possibility also exists that glycine and GABA may be co-released from the same presynaptic terminals of inhibitory interneurons (Jonas et al. 1998). Whether the excitability of lumbar glycinergic or GABAergic (inter)neurons that are coupled to DSCT neurons depends on behavioral state requires additional studies.

Reticulospinal neurons may also form part of the corticofugal pathway(s) that impinges on DSCT neurons via synaptic linkages with inhibitory interneurons (Hongo et al. 1983; Jankowska 1992; Rudomin et al. 1990; Takakusaki et al. 2001). During REM sleep, these inhibitory influences would be strengthened due to the increased firing rate of reticulospinal neurons (Taepavarapruk et al. 2003; Wyzinski et al. 1978). Additional evidence in support of this proposed neuronal circuit is derived from the present study where electrical stimulation of the NRGc during the state of wakefulness evoked the release of glutamate and glycine, but not GABA, in the L_3 spinal gray matter at stimulation intensities sufficient to suppress cerebellar-driven field potentials reflecting inhibition of DSCT neurons.

During REM sleep, reticulospinal neurons in the NRGc display marked increases in their discharge rates whereas simultaneously recorded DSCT neurons undergo decreased firing rates (Taepavarapruk et al. 2003) mediated by glycine (Taepavarapruk et al. 2002). In the present study, the finding that NRGc stimulation increased spinal glutamate and glycine levels suggests that a portion of the suppressor influences arising from NRGc stimulation on DSCT neurons is due to the release of glycine. Kodama et al. (2003) also reported that electrical stimulation of the pontine inhibitory area increased glycine and GABA concentrations modestly by 26 and 12%, respectively, in the ventral horn.

Dopamine

The source of dopamine (DA) in the spinal cord arises from neurons (A11 cell group) located in the diencephalon (Cechetto and Saper 1988; Holstege et al. 1996). In the present study, dopamine levels in the spinal cord were significantly decreased by 28% during REM sleep compared with wakefulness. NRGc stimulation failed to alter dopamine levels during wakefulness, a finding that implies a supraspinal origin for spinal DA that is distinct from the amino acids glutamate and glycine. The decrease in DA levels during REM sleep may occur as a result of REM sleep-dependent reductions in the excitability of A11-DA neurons projecting to the cord. Diencephalospinal A11-DA neurons may therefore be distinct from substantia nigra neurons or dopaminergic neurons in the ventral tegmental area whose firing rates do not differ across the wake–sleep cycle (Steinfels et al. 1983; Trulson and Preussler 1984; Trulson et al. 1981). Alternatively, the REM sleep-related decrease in spinal DA levels could arise as a consequence of enhanced (or reduced) terminal excitability of A11 centrifugally projecting dopaminergic neurons (Maitra et al. 1992; Yang and Mogenson 1986). Electrophysiological studies of A11 diencephalospinal DA neurons across the wake-sleep cycle are needed to distinguish between these possibilities.

Implications for the sensorimotor disorder of restless legs syndrome

The tonic release of DA in the spinal cord during naturally occurring wakefulness and NREM sleep in intact animals reported here may infer that A11-DA neurons exert an executive role in protecting against restless legs syndrome (RLS), a sleep disorder characterized by an irresistible urge to move one's legs to relieve unpleasant sensory dysesthesias. The sensory dysesthesias of RLS are managed, in part, by dopaminergic drugs and are thought to be triggered by disinhibition of spinal sensory tract neurons due to compromised dopamine neurons in the brain (e.g., A11 cell group) (Clemens et al. 2006). Indeed, recent findings in our laboratories have indicated that when the A11-DA cell groups are ablated by the neurotoxin 6-OHDA, sensory thresholds in awake rats are markedly and permanently reduced along with spinal cord levels of DA (Wang et al. 2005). Although the actions of microiontophoretic DA (ant)agonists on individual DSCT and SRT neurons have yet to be reported, D_2 receptors do mediate inhibition of nociceptor-driven responses of rat spinothalamic

tract and cat spinocervical tract neurons (Fleetwood-Walker et al. 1988). DSCT and SRT neurons would be reasonable candidate sensory tract neurons that may convey sensory dysesthesias if diencephalospinal A11-DA neurons are compromised in RLS since these neurons receive an array of muscular and cutaneous afferent inputs from lower limb dermatomes and also project to higher brain centers including the thalamus (Bosco and Poppele 2001; Lu and Willis 1999).

Taken together, these converging lines of evidence suggest that under normal conditions, A11-DA neurons may provide a tonic dopaminergic inhibitory input to spinal cord sensory neurons during wakefulness and NREM sleep, which, during REM sleep, is not only diminished but also compensated for by increased inhibition afforded by other glycine and GABAergic neural networks discussed earlier. If A11-DA diencephalospinal neurons become dysfunctional in RLS, such an imbalance in the release of dopamine in the spinal cord during wakefulness just prior to the onset of sleep may contribute to the sensory dysesthesias experienced by RLS patients and, perhaps, even so in patients suffering from various forms of chronic pain (Soja 2007).

REFERENCES

Bosco G, Poppele RE. Proprioception from a spinocerebellar perspective. *Physiol Rev* 81: 539–568, 2001.

Buchanan JT, Grillner S. Newly identified "glutamate interneurons" and their role in locomotion in the lamprey spinal cord. *Science* 236: 312–314, 1987.

Cechetto DF, Saper CB. Neurochemical organization of the hypothalamic projection to the spinal cord in the rat. *J Comp Neurol* 272: 579–604, 1988.

Chandler MJ, Garrison DW, Brennan TJ, Foreman RD. Effects of chemical and electrical stimulation of the midbrain on feline T2–T6 spinoreticular and spinal cell activity evoked by cardiopulmonary afferent input. *Brain Res* 496: 148–164, 1989.

Chase MH, Morales FR. The atonia and myoclonia of active (REM) sleep. *Annu Rev Psychol* 41: 557–584, 1990.

Chase MH, Morales FR, Boxer PA, Fung SJ, Soja PJ. Effect of stimulation of the nucleus reticularis gigantocellularis on the membrane potential of cat lumbar motoneurons during sleep and wakefulness. *Brain Res* 386: 237–244, 1986.

Clemens S, Rye D, Hochman S. Restless legs syndrome: revisiting the dopamine hypothesis from the spinal cord perspective. *Neurology* 67: 125–130, 2006.

Curtis DR, Gynther BD, Malik R. A pharmacological study of group I muscle afferent terminals and synaptic excitation in the intermediate nucleus and Clarke's column of the cat spinal cord. *Exp Brain Res* 64: 105–113, 1986.

Curtis DR, Hosli L, Johnston GA. A pharmacological study of the depression of spinal neurones by glycine and related amino acids. *Exp Brain Res* 6: 1–18, 1968.

Curtis DR, Phillis JW. gamma-Amino-*n*-butyric acid and spinal synaptic transmission (Letter). *Nature* 182: 323, 1958.

Fleetwood-Walker SM, Hope PJ, Mitchell R. Antinociceptive actions of descending dopaminergic tracts on cat and rat dorsal horn somatosensory neurones. *J Physiol* 399: 335–348, 1988.

Holstege JC, Bongers CM. A glycinergic projection from the ventromedial lower brainstem to spinal motoneurons. An ultrastructural double labeling study in rat. *Brain Res* 566: 308–315, 1991.

Holstege JC, Van Dijken H, Buijs RM, Goedknegt H, Gosens T, Bongers CM. Distribution of dopamine immunoreactivity in the rat, cat and monkey spinal cord. *J Comp Neurol* 376: 631–652, 1996.

Hongo T, Jankowska E, Ohno T, Sasaki S, Yamashita M, Yoshida K. The same interneurones mediate inhibition of dorsal spinocerebellar tract cells and lumbar motoneurones in the cat. *J Physiol* 342: 161–180, 1983.

Jankowska E. Interneuronal relay in spinal pathways from proprioceptors. *Prog Neurobiol* 38: 335–378, 1992.

John J, Wu MF, Kodama T, Siegel JM. Intravenously administered hypocretin-1 alters brain amino acid release: an in vivo microdialysis study in rats. *J Physiol* 548: 557–562, 2003.

Jonas P, Bischofberger J, Sandkuhler J. Corelease of two fast neurotransmitters at a central synapse. *Science* 281: 419–424, 1998.

Jones BE, Holmes CJ, Rodriguez-Veiga E, Mainville L. GABA-synthesizing neurons in the medulla: their relationship to serotonin-containing and spinally projecting neurons in the rat. *J Comp Neurol* 313: 349–367, 1991.

Kodama T, Lai YY, Siegel JM. Changes in inhibitory amino acid release linked to pontine-induced atonia: an in vivo microdialysis study. *J Neurosci* 23: 1548–1554, 2003.

Kubota S, Poppele RE. Evidence for control of DSCT activity by the brain stem reticular formation. *Brain Res* 129: 361–365, 1977.

Lai YY, Kodama T, Siegel JM. Changes in monoamine release in the ventral horn and hypoglossal nucleus linked to pontine inhibition of muscle tone: an in vivo microdialysis study. *J Neurosci* 21: 7384–7391, 2001.

Linderoth B, Stiller CO, Gunasekera L, O'Connor WT, Ungerstedt U, Brodin E. Gamma-aminobutyric acid is released in the dorsal horn by electrical spinal cord stimulation: an in vivo microdialysis study in the rat. *Neurosurgery* 34: 484–488; discussion 488–489, 1994.

Lu GW, Willis WD. Branching and/or collateral projections of spinal dorsal horn neurons. *Brain Res Brain Res Rev* 29: 50–82, 1999.

Magoul R, Onteniente B, Geffard M, Calas A. Anatomical distribution and ultrastructural organization of the GABAergic system in the rat spinal cord. An immunocytochemical study using anti-GABA antibodies. *Neuroscience* 20: 1001–1009, 1987.

Maitra KK, Seth P, Ross HG, Thewissen M, Ganguly DK. Presynaptic dopaminergic inhibition of the spinal reflex in rats. *Brain Res Bull* 28: 817–819, 1992.

Maxwell DJ, Christie WM, Ottersen OP, Storm-Mathisen J. Terminals of group Ia primary afferent fibres in Clarke's column are enriched with L-glutamate-like immunoreactivity. *Brain Res* 510: 346–350, 1990.

Ornung G, Shupliakov O, Ottersen OP, Storm-Mathisen J, Cullheim S. Immunohistochemical evidence for coexistence of glycine and GABA in nerve terminals on cat spinal motoneurones: an ultrastructural study. *Neuroreport* 5: 889–892, 1994.

Pilowsky PM, Kapoor V, Minson JB, West MJ, Chalmers JP. Spinal cord serotonin release and raised blood pressure after brainstem kainic acid injection. *Brain Res* 366: 354–357, 1986.

Rudomin P, Jimenez I, Quevedo J, Solodkin M. Pharmacologic analysis of inhibition produced by last-order intermediate nucleus interneurons mediating nonreciprocal inhibition of motoneurons in cat spinal cord. *J Neurophysiol* 63: 147–160, 1990.

Soja P. Modulation of prethalamic sensory inflow during sleep versus wakefulness. In: *Sleep and Pain*, edited by Lavigne G, Sessle B, Choiniere M, Soja P. Seattle, WA: IASP Press, 2007, p. 45–76.

Soja PJ, Fragoso MC, Cairns BE, Jia WG. Dorsal spinocerebellar tract neurons in the chronic intact cat during wakefulness and sleep: analysis of spontaneous spike activity. *J Neurosci* 16: 1260–1272, 1996.

Soja PJ, Fragoso MC, Cairns BE, Oka JI. Dorsal spinocerebellar tract neuronal activity in the intact chronic cat. *J Neurosci Methods* 60: 227–239, 1995a.

Soja PJ, Lopez-Rodriguez F, Morales FR, Chase MH. The postsynaptic inhibitory control of lumbar motoneurons during the atonia of active sleep: effect of strychnine on motoneuron properties. *J Neurosci* 11: 2804–2811, 1991.

Soja PJ, Lopez-Rodriguez F, Morales FR, Chase MH. Effects of excitatory amino acid antagonists on the phasic depolarizing events that occur in lumbar motoneurons during REM periods of active sleep. *J Neurosci* 15: 4068–4076, 1995b.

Soja PJ, Morales FR, Baranyi A, Chase MH. Effect of inhibitory amino acid antagonists on IPSPs induced in lumbar motoneurons upon stimulation of the nucleus reticularis gigantocellularis during active sleep. *Brain Res* 423: 353–358, 1987.

Soja PJ, Pang W, Taepavarapruk N, Cairns BE, McErlane SA. On the reduction of spontaneous and glutamate-driven spinocerebellar and spino-

reticular tract neuronal activity during active sleep. *Neuroscience* 104: 199–206, 2001a.

Soja PJ, Pang W, Taepavarapruk N, McErlane SA. Spontaneous spike activity of spinoreticular tract neurons during sleep and wakefulness. *Sleep* 24: 18–25, 2001b.

Solodkin M, Jimenez I, Rudomin P. Identification of common interneurons mediating pre- and postsynaptic inhibition in the cat spinal cord. *Science* 224: 1453–1456, 1984.

Sorkin LS, McAdoo DJ. Amino acids and serotonin are released into the lumbar spinal cord of the anesthetized cat following intradermal capsaicin injections. *Brain Res* 607: 89–98, 1993.

Sorkin LS, McAdoo DJ, Willis WD. Raphe magnus stimulation-induced antinociception in the cat is associated with release of amino acids as well as serotonin in the lumbar dorsal horn. *Brain Res* 618: 95–108, 1993.

Steinfels GF, Heym J, Strecker RE, Jacobs BL. Response of dopaminergic neurons in cat to auditory stimuli presented across the sleep-waking cycle. *Brain Res* 277: 150–154, 1983.

Taepavarapruk N, McErlane S, Soja P. Reciprocal state-dependent changes in reticulospinal (RS) and dorsal spinocerebellar tract (DSCT) neuron activity. Program No. 499.417. *2003 Abstract Viewer and Itinerary Planner*. Washington, DC: Society for Neuroscience, 2003. Online.

Taepavarapruk N, McErlane SA, Chan A, Chow S, Fabian L, Soja PJ. State-dependent GABAergic inhibition of sciatic nerve-evoked responses of dorsal spinocerebellar tract neurons. *J Neurophysiol* 92: 1479–1490, 2004.

Taepavarapruk N, McErlane SA, Soja PJ. State-related inhibition by GABA and glycine of transmission in Clarke's column. *J Neurosci* 22: 5777–5788, 2002.

Taepavarapruk P, Phillips AG. Neurochemical correlates of relapse to d-amphetamine self-administration by rats induced by stimulation of the ventral subiculum. *Psychopharmacology* (*Berl*) 168: 99–108, 2003.

Takakusaki K, Kohyama J, Matsuyama K, Mori S. Medullary reticulospinal tract mediating the generalized motor inhibition in cats: parallel inhibitory mechanisms acting on motoneurons and on interneuronal transmission in reflex pathways. *Neuroscience* 103: 511–527, 2001.

Trulson ME, Preussler DW. Dopamine-containing ventral tegmental area neurons in freely moving cats: activity during the sleep-waking cycle and effects of stress. *Exp Neurol* 83: 367–377, 1984.

Trulson ME, Preussler DW, Howell GA. Activity of substantia nigra units across the sleep-waking cycle in freely moving cats. *Neurosci Lett* 26: 183–188, 1981.

Vesselkin NP, Rio JP, Adanina VO, Kenigfest NB, Reperant J. Colocalization of glutamate and glycine in giant fiber synapses of the lamprey spinal cord. *J Hirnforsch* 36: 229–237, 1995.

Walmsley B, Nicol MJ. The effects of Ca^{2+}, Mg^{2+} and kynurenate on primary afferent synaptic potentials evoked in cat spinal cord neurones in vivo. *J Physiol* 433: 409–420, 1991.

Wang D, Sutherland D, McErlane S, Soja P. Long-lasting reduction in rat sensory thresholds following ablation of diencephalic A11 dopamine (DA) nuclei. *Soc Neurosci* 623.21, 2005.

Wannier T, Orlovsky G, Grillner S. Reticulospinal neurones provide monosynaptic glycinergic inhibition of spinal neurones in lamprey. *Neuroreport* 6: 1597–1600, 1995.

Watson AH, Bazzaz AA. GABA and glycine-like immunoreactivity at axo-axonic synapses on 1a muscle afferent terminals in the spinal cord of the rat. *J Comp Neurol* 433: 335–348, 2001.

Werman R. Criteria for identification of a central nervous system transmitter. *Comp Biochem Physiol* 18: 745–766, 1966.

Wyzinski PW, McCarley RW, Hobson JA. Discharge properties of pontine reticulospinal neurons during sleep-waking cycle. *J Neurophysiol* 41: 821–834, 1978.

Yang CR, Mogenson GJ. Dopamine enhances terminal excitability of hippocampal-accumbens neurons via D2 receptor: role of dopamine in presynaptic inhibition. *J Neurosci* 6: 2470–2478, 1986.